J Mater Sci (2012) 47:412–419
DOI 10.1007/s10853-011-5814-z

Polymer grafting onto magnetite nanoparticles by "click" reaction

J. Amici · M. U. Kahveci · P. Allia · P. Tiberto · Y. Yagci · M. Sangermano

Received: 11 May 2011 / Accepted: 21 July 2011 / Published online: 30 July 2011

Abstract In this article, we described click chemistry methodology for the incorporation of biocompatible polymer chains to Magnetite nanoparticles (NPs). We used a reduction co-precipitation method to obtain Fe_3O_4 particles in aqueous solution. As a next step, magnetic NPs surface were modified by a silanization reaction with (3-bromopropyl)trimethoxysilane in order to introduce bromine groups on the particles surface which were converted to azide groups by the reaction with sodium azide. Acetylene functionalized poly(ethylene glycol) (**a**-PEG) and poly-(ε-caprolactone) (**a**-PCL) were synthesized and grafted onto the surface of azide functionalized NPs via "click" reaction to obtain magnetic NPs. Success of the different functionalization processes at different stages was studied using Fourier Transform infrared spectroscopy (FTIR). The morphologies of magnetic NPs were further investigated by transmission electron microscopy (TEM). The magnetization and superparamagnetic behavior of naked Fe_3O_4 NPs and coated NPs at room temperature was investigated by the measurement of hysteresis curves using a Vibrating Sample Magnetometer (VSM).

J. Amici · P. Allia · M. Sangermano (✉)
Dipartimento di Scienza dei Materiali e Ingegneria Chimica, Politecnico di Torino, Corso Duca degli Abruzzi 24, 10125 Turin, Italy
e-mail: marco.sangermano@polito.it

M. U. Kahveci · Y. Yagci
Department of Chemistry, Istanbul Technical University, Maslak, 34469 Istanbul, Turkey

P. Tiberto
INRIM, Electromagnetism, Strada delle Cacce 91, 10135 Turin, Italy

Introduction

It is widely reported in literature that targeted hyperthermia is a highly suitable technique for cancer therapy [1–3], since tumor cells are highly susceptible to elevated temperatures. If tumor cells are heated up to 41–45 °C, the tissue damage for normal tissue is reversible while the tumor cells are irreversibly damaged [4]. Superparamagnetic particles exposed to an alternating magnetic field can be used for heat induction and are therefore a good candidate for hyperthermia. Superparamagnetic iron oxide nanoparticles (SPION) are small synthetic Fe_2O_3 or Fe_3O_4 particles with a core size of 10 nm and an organic or inorganic shell. After eliminating the magnetic field, superparamagnetic particles no longer show magnetic interaction; a feature that is important for their usability. SPION have a much higher rate of specific absorption compared with larger magnetic particles with several magnetic domains and therefore, are predestinated for use in hyperthermia [5–7]. The possibilities of SPION applications have drastically increased in recent years [8–10]. In the clinical area of human medicine, these particles are being used as delivery systems for drugs [11–13], genes [14], and radionuclides [15]. Furthermore, ferrofluids, as contrast agents in magnetic resonance imaging (MRI), are routinely applied in the field of diagnostic imaging [16–18]. SPION are also attractive for in vitro applications in medical diagnostics, such as research in genetics and technologies based on immune magnetic separation (IMS) of cells, proteins, DNA/RNA, bacteria, virus, and other biomolecules [19].These particles are typically coated with a biocompatible polymer-shell to prevent their aggregation and biodegradation for in vivo applications [20–23]. Furthermore, in the case of intravenous administration the coating as well as the dimension of nanoparticles are essential to avoid the recognition and uptake by the mononuclear phagocyte system

(MPS) followed by clearance to the liver, spleen, and bone marrow by the reticuloendothelial system (RES).Taking all these aspects in mind, it is clear the great challenge in the synthesis of magnetic-polymer core–shell nanoparticles (NPs) for bio-medical applications. To face this challenge, we thought to use click-reaction for magnetite surface functionalization. "Click chemistry" focuses on the extraordinary power of a very few reactions which form desired bonds under diverse reaction conditions, with highly diverse building blocks, in high yields and with no byproducts [24, 25]. Recent studies demonstrated that "click" chemistry meets the criteria of being applicable under aqueous conditions, efficient, orthogonal to thiol- and amine-containing targeting motifs, and stable in the complex in vivo environments of the blood and tumor milieu [26]. Click reaction has been already proposed for the surface functionalization of gold NPs [27] and silica NPs [28].

In this study, we report the use of "click" reactions for preparing magnetic NPs with Fe_3O_4 core and different biocompatible polymeric shells. We used a reduction co-precipitation method to obtain Fe_3O_4 particles in aqueous solution. As a next step, magnetic NPs surface has been modified by a silanization reaction with (3-bromopropyl)trimethoxysilane in order to introduce bromine groups on the particles surface. Afterward the bromine groups were converted to azide groups by the reaction with sodium azide in order to obtain azide groups to take part to click reaction with alkyne functionalized polymers. For this reason, acetylene functionalized poly(ethylene glycol) (**a**-PEG) and poly(ε-caprolactone) (**a**-PCL) were synthesized and grafted onto the surface of azide functionalized NPs via "click" reaction to obtain polymer-coated magnetic NPs. These polymers were deliberately selected so as to introduce biocompatible macromolecular chains, and the peculiar characteristics of this method make it ideal for biomedical applications.

Success of the different functionalization processes at different stages was studied using Fourier Transform infrared spectroscopy (FTIR). The morphologies of magnetic NPs were further investigated by transmission electron microscopy (TEM). The magnetization and superparamagnetic behavior of naked Fe_3O_4 NPs and coated NPs at room temperature was investigated by the measurement of hysteresis curves using a Vibrating Sample Magnetometer (VSM).

Experimental part

Materials

Ethanol (99.9%, Labochem), acetic acid (≥99.7%, Sigma-Aldrich), (3-bromopropyl)trimethoxysilane (≥97.0%, Aldrich), tin(II) 2-ethylhexanoate (95%, Aldrich), propargyl alcohol (99%, Aldrich), 4-pentynoic acid (98%, Alfa Aesar), *N,N′*-dicyclohexylcarbodiimide (DCC, 99%, Aldrich), 4-dimethylaminopyridine (DMAP, 99%, Aldrich), sodium azide (NaN_3, 99%, Acros), CuBr (98%, Acros), *N,N,N′,N″,N″*-pentamethyldiethylenetriamine (PMDETA, 99%, Aldrich), poly(ethylene glycol)monomethylether (PEG, M_n: 2000, Fluka), $FeCl_3{\cdot}6H_2O$ (97%, Sigma-Aldrich) were used as received. ε-Caprolatone (ε-CL) was distilled under vacuum over CaH_2. *N,N*-Dimethyl formamide (DMF) and dichloromethane (99%, CH_2Cl_2, J. T. Baker) were previously dried and distilled over phosphorus pentoxide.

Synthesis of acetylene end-functionalized PCL

Poly(ε-caprolactone) with alkyne end-functionality (a-PCL) was prepared by Ring Opening Polymerization of ε-CL (5.0 mL; 0.047 mol) in bulk using tin(II) 2-ethylhexanoate as a catalyst (catalytic amount) and propargyl alcohol (0.102 mL; 1.175 mmol) as an initiator. The monomer, catalyst, and initiator were added to a previously flamed Schlenk tube equipped with a magnetic stirring bar in the order mentioned. The tube was degassed with three freeze–pump–thaw cycles, left under nitrogen, and placed in a thermostated oil bath at 110 °C for 18 h. After the polymerization, the mixture was diluted with THF and precipitated into an excess amount of methanol. Then, it was filtrated (filter pore ŋ4) and dried overnight at room temperature under vacuum. $[M]_0/[I]_0 = 40$; conversion = 67%; $M_{n,theo} = 3100$; $M_{n,NMR} = 1613$; $M_{n,GPC} = 6000$ (relative to linear polystyrene); $M_w/M_n = 1.11$. ^{1}H NMR ($CDCl_3$,δ): 4.66 (2H, CH≡C–CH_2O), 4.03 (2H, CH_2OC=O of PCL), 3.62 (2H, CH_2OH, end group of PCL), 2.28 (2H, C=OCH_2 of PCL), 1.20–1.80 (6H, CH_2 of PCL). The schematic synthesis is depicted in Fig. 1.

Synthesis of acetylene end-functionalized PEG

Mono hydroxyl functional PEG (M_n: 2000 g/mol, 3.0 g, 1.5 mmol) was dissolved in 25 mL of dry CH_2Cl_2, and 4-pentynoic acid (0.22 g, 2.25 mmol) and DMAP (0.18 g, 1.5 mmol) were successively added to the reaction mixture. After stirring for 5 min at room temperature, a solution of DCC (0.46 g, 2.25 mmol) in 15 mL of CH_2Cl_2 was added to the reaction mixture and stirred overnight at room temperature. After filtration of the salt, the solution was

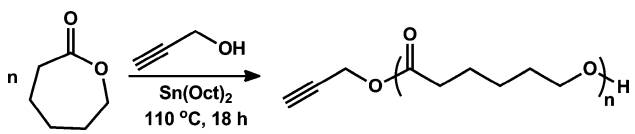

Fig. 1 Synthesis of a-PCL by Ring Opening Polymerization

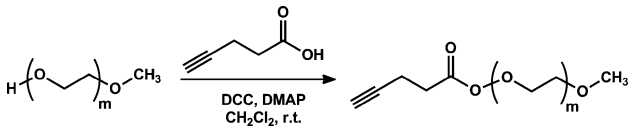

Fig. 2 Synthesis of a-PEG

concentrated and the product was purified by column chromatography over silica gel eluting with CH_2Cl_2/ethyl acetate mixture (1:10) and then with CH_2Cl_2/MeOH (10:1). Finally, concentrated solution of acetylene end-functionalized PEG (a-PEG) was precipitated in diethyl ether and filtered. $M_{n,theo} = 2100$; $M_{n,NMR} = 1483$; $M_{n,GPC} = 2400$ (relative to linear polystyrene); $M_w/M_n = 1.08$. ^{1}H NMR ($CDCl_3$,δ): 4.21 (t, 2H, PEG-OCH_2CH_2–OC=O), 3.70–3.50 (m, 8H, PEG-OCH_2CH_2OC=O, –OCH_2CH_2– of PEG, and CH_2CH_2–O–CH_3), 3.32 (s, 3H, CH_3–OCH_2CH_2). 2.53–2.45 (m, 4H, CH≡CCH_2CH_2C=O), 1.94 (t, 1H, CH≡CCH_2–CH_2C=O). The schematic synthesis is depicted in Fig. 2.

Synthesis of magnetite NPs

Magnetite nanoparticles (NPs) were synthesized by a chemical co-precipitation of Fe^{2+} and Fe^{3+} ions under alkaline conditions, as already reported in literature [3]. As a typical procedure, 3.25 g of $FeCl_3 \cdot 6H_2O$ was dissolved into 100 mL of distilled water. The solution was added into a three-necked flask together with 5 mL of Na_2SO_3 solution at 5 wt%. Subsequently, 20 mL of concentrated ammonia were diluted into 40 mL of distilled water, and then added into the flask under nitrogen inlet; the solution quickly turned black. The solution was stirred for 30 min at 70 °C. Following the temperature solution was raised up to 95 °C and 1 g of citric acid was added dissolved into 2 mL of water. After 90 min, the solution was cooled down to room temperature. The black precipitate was separated with a magnet and washed several times with distilled water. The Fe_3O_4 NPs were redispersed in distilled water. The water dispersion of Fe_3O_4 NPs showed superparamagnetic property, as measurements from a previous study [29]. The magnetite concentration was 14 mg/mL, as determined by TGA analyses.

Functionalization of magnetite NPs with (3-bromopropyl)trimethoxysilane

Acetic acid (3 mL), 3-(bromopropyl)trimethoxysilane (0.239 mL), and magnetic NPs (74 mg) were added to a solution of water and ethanol (1:10 vol/vol). The solution was left under magnetic stirring for 24 h at room temperature. The black precipitate was separated with a magnet and washed several times with distilled water. The Fe_3O_4 NPs were redispersed in distilled water. The concentration of bromo functional magnetite NPs (Fe_3O_4–AC–Br NPs) aqueous dispersion was determined by means of TGA to be 6.0 mg/mL.

Azidation of bromine-functionalized magnetite NPs

Fe_3O_4–AC–Br NPs in aqueous solution (10 mL) were added to a flask containing a large excess of sodium azide (100 mg, ~13 equiv. Br). The solution was left under stirring at room temperature for 48 h. The azidation process was stopped by centrifugation of the solution. The sample was centrifuged three times at 5000 rpm for 20 min and washed with water. Successively, the pellet containing azido functional magnetite (Fe_3O_4–AC–N_3) nanoparticles was dried at room temperature for 48 h.

Grafting of PCL onto magnetite NPs

a-PCL (55.8 mg, 1 equiv.), CuBr (3.9 mg, 1.5 equiv.), and 2 mL of DMF were added in a Schlenk tube. 10 mg of the magnetic NPs (0.9 equiv. N_3) were dispersed in 3 mL of DMF and added to the tube. Finally, PMDETA (5.8 μL, 1.5 equiv.) was added to the solution. The tube was degassed with three freeze–pump–thaw cycles, left under vacuum and put in a thermostated bath at 50 °C for 48 h. In order to stop the reaction, the solution was centrifuged at 5000 rpm for 30 min, then the supernatant was removed and the NPs were washed with toluene. The solution was centrifuged again at 5000 rpm for 30 min. This process was repeated two times with toluene and one time with water in order to remove unreacted polymer and copper catalyst. Successively, the NPs (Fe_3O_4–AC–N_3 NPs) were dried for 48 h at room temperature.

Grafting of PEG onto magnetite NPs

Alkyne-PEG (22.5 mg, 1 equiv.) and CuBr (2.6 mg, 1.5 equiv.) were dissolved in 2 mL of DMF in a Schlenck tube. 8.2 mg of Fe_3O_4–AC–N_3 NPs (1.2 equiv. N_3) and PMDETA (3.7 μL, 1.5 equiv.) were added to the solution. The tube was degassed with three freeze–pump–thaw cycles, left under vacuum and put in a thermostated bath at 50 °C for 48 h. In order to stop the reaction, the solution was centrifuged at 5000 rpm for 30 min. The pellet dispersed in 0.5 mL of THF and precipitated in 5 mL of cold distilled water, then two drops of hydrochloric acid were added to the solution and the solution was put at 4 °C for 4 h. The supernatant solution was removed and the NPs were dried under vacuum at room temperature overnight.

Characterization techniques

^{1}H NMR spectra of 5–10% (w/w) solutions in $CDCl_3$ with $Si(CH_3)_4$ as an internal standard were recorded at room

temperature at 250 MHz on a Bruker DPX 250 spectrometer. Gel permeation chromatography (GPC) measurements were obtained from a Viscotek GPC max Autosampler system consisting of a pump, a Viscotek UV detector, and a differential refractive index detector. Tetrahydrofuran (THF) was used as an eluent at flow rate of 1.0 mL min^{-1} at 30 °C. Molecular weights of the a-PCL and a-PEG were determined with the aid of polystyrene standards. Fourier transform infrared (FTIR) spectra were recorded on a Perkin-Elmer FTIR Spectrum One B spectrometer. Thermogravimetric analysis (TGA) was performed on a Perkin-Elmer Diamond TA/TGA instrument at a heating rate of 10 °C min^{-1} under nitrogen flow.

Magnetic hysteresis loops were measured at room temperatures on coated magnetite water dispersion using a vibrating sample magnetometer (VSM) operating in the magnetic field range -10 kOe $< H < +10$ kOe. The diamagnetic contribution of sample holder and solvent were significant. A reference measurement was preliminarily done by measuring the magnetic response of the sample holder filled with the same amount of pure solvent (i.e., without the magnetic NPs). The magnetic contribution ascribed to magnetite NPs (before and after functionalization) was obtained from the measured curves by subtracting the reference curve.

Samples were observed using TEM by examining in a 300 keV Philips CM30 instrument. TEM micrographs were processed with a slow scan CCD camera and analyzed with the Digital Micrograph program. The TEM observations were always performed using a very low electron flux in order to avoid any structural modification of the sample induced by the electron beam.

Results and discussion

In this article, we aim to show the use of "click chemistry" for the preparation of magnetite-core/polymer-shell NPs. The overall strategy, as presented in Scheme 1, is based firstly on the preparation of bromine-functionalized magnetite NPs, and then after azidation, the NPs are functionalized via click-reaction either with PCL or PEG polymeric shells.

Magnetite NPs were synthesized by a chemical co-precipitation of Fe^{2+} and Fe^{3+} ions under alkaline conditions, following previous method reported in literature [30–35]. Citric acid was added during the synthesis in order to protect the NPs avoiding macroscopic aggregations. The magnetite NPs, prepared with the co-precipitation method, were functionalized with bromine groups using 3-(bromopropyl)trimethoxysilane (see Scheme 1). Modified magnetite NPs were characterized by FTIR spectroscopy. In Fig. 3, the FTIR spectra are reported for bare Fe_3O_4 NPs (spectrum A) and bromine functionalized Fe_3O_4 NPs (spectrum B), respectively. In the spectrum B, it can be seen that the strong and broad peak centered at around 3100 cm^{-1} disappeared, while a peak centered at around 1112 cm^{-1} appeared after reactive functionalization of the NPs. The disappearance of the peak centered at 3100 cm^{-1}

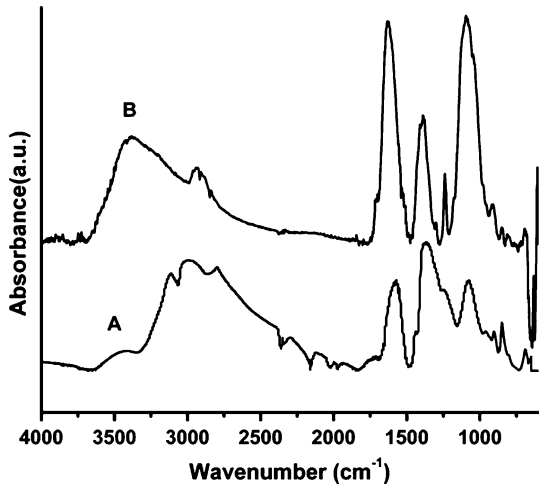

Fig. 3 FTIR spectra of bare magnetite nanoparticles (curve *A*) and bromine functionalized nanoparticles (curve *B*)

Scheme 1 Overall strategy of magnetite functionalization via "click" reaction

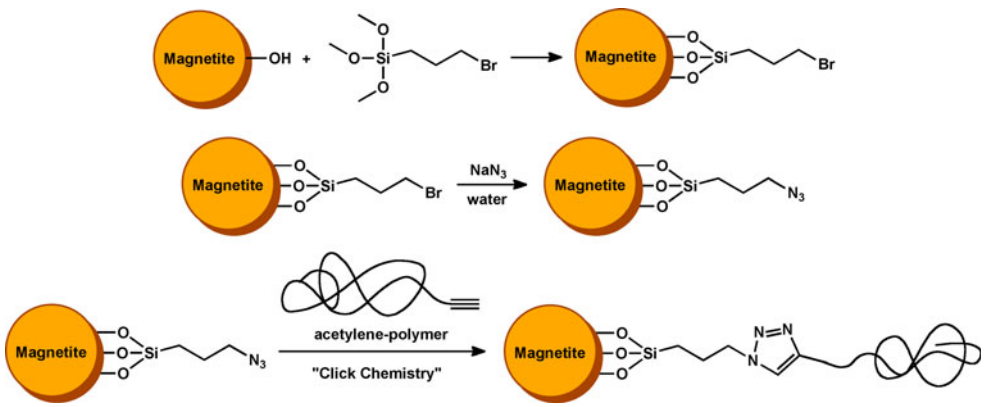

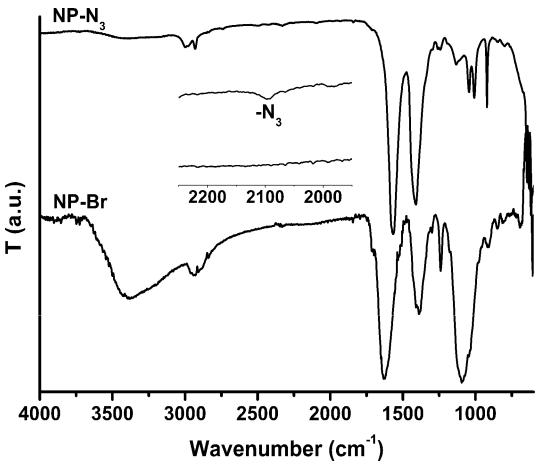

Fig. 4 FTIR spectra of the magnetic nanoparticles before (NP-Br) and after (NP-N_3) azidation, zoom on the azide peak region

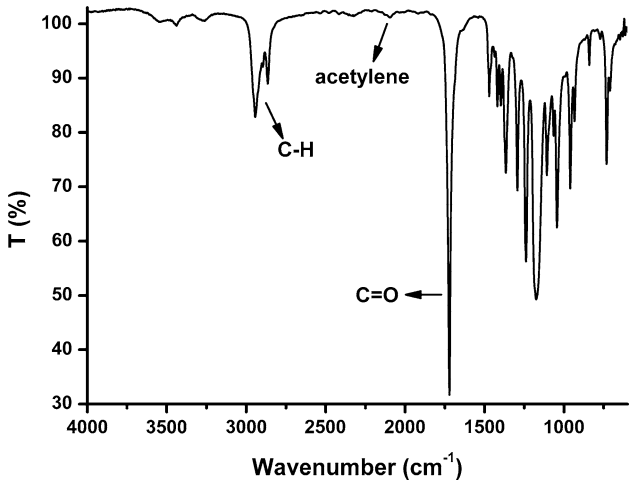

Fig. 5 FTIR spectrum of a-PCL

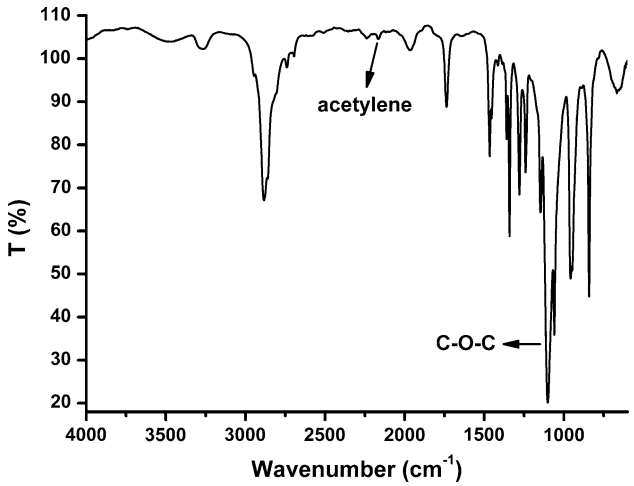

Fig. 6 FTIR spectrum of a-PEG

can be attributed to the consumption of the hydroxyl groups present on the surface of Fe_3O_4 NPs, during the silanization reaction, while the appearance of the peak centered at 1112 cm^{-1} can be attributed to the C–O–Si stretching band.

The bromine-functionalized magnetite NPs were used as the precursor materials for the "click" modification by conversion to an azide-functional surface through nucleophilic substitution. Actually, the nanoparticules were azidated by the substitution of the bromine groups with sodium azide. The successful azidation was confirmed by ATR analysis. In Fig. 4, the IR spectra of both the bromine functionalized NPs and azide functionalized NPs are reported with a zoom on the azide peak region. The azidation of the NPs was confirmed by the appearance of the peak centered at 2100 cm^{-1} characteristic of the azide group.

For the subsequent click modification, alkyne-PCL and alkyne-PEG were synthesized as described in the experimental part. In particular, as presented in Fig. 1, the alkyne-PCL (a-PCL) was prepared by Ring Opening Polymerization (ROP) of ε-CL in bulk using tin(II) 2-ethylhexanoate as a catalyst and propargyl alcohol as an initiator. The alkyne PCL was further characterized by ATR spectroscopy. As can be seen in Fig. 5, the successful synthesis of alkyne-PCL was confirmed by the alkyne stretching band around 2150 cm^{-1} and the typical bands of PCL, such as C=O stretching at 1730 cm^{-1}, asymmetric C–O–C stretching at 1241 cm^{-1} or C–C stretching at 1047 cm^{-1}.

Regarding the alkyne-PEG (a-PEG), it was synthesized by the esterification reaction between 4-pentynoic acid and monohydroxyl functional PEG in CH_2Cl_2 (reaction scheme illustrated in Fig. 2). The a-PEG was further characterized by ATR spectroscopy. As can be seen in Fig. 6, the successful synthesis of a-PEG was confirmed by the alkyne stretching band around 2150 cm^{-1} and the typical bands of PEG, such as C–O–C vibration around 1100 cm^{-1} and out-of-plane bending of the –CH of the chain at 960 cm^{-1}.

The polymer functionalized NPs were characterized by ATR spectroscopy. Figure 7 shows the spectra of azide functional NPs (NP-N_3), a-PCL, and a-PCL functionalized magnetic NPs (NP-PCL). As can be seen from the first and second spectra, the azide peak around 2100 cm^{-1} and the alkyne peak around 2150 cm^{-1}, respectively, disappeared confirming the reaction between the azide group and the alkyne group. The functionalization is further confirmed by the presence on the third spectrum (NP-PCL) of the typical peaks of PCL, such as C=O stretching at 1730 cm^{-1}, asymmetric C–O–C stretching at 1241 cm^{-1} or C–C stretching at 1047 cm^{-1} and the disappearance of the alkyne stretching band at 2150 cm^{-1}. The degree of functionalization of the magnetite particles was evaluated

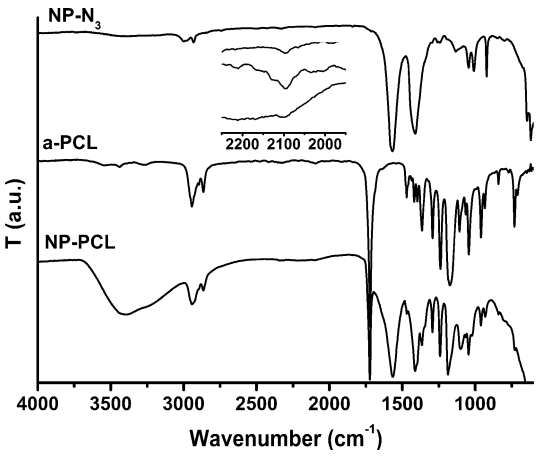

Fig. 7 FTIR spectrum of azide functionalized nanoparticles (NP-N_3), a-PCL, and PCL functionalized nanoparticles (NP-PCL)

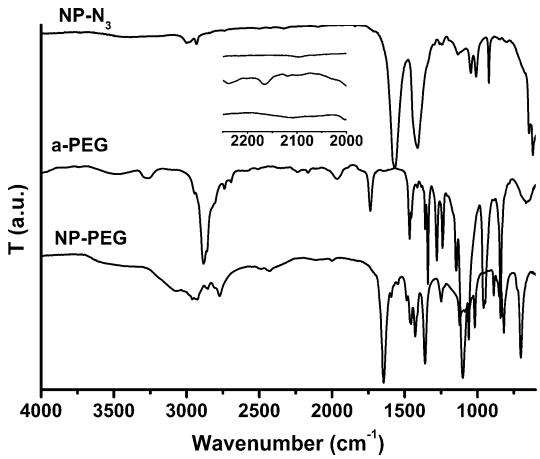

Fig. 9 FTIR spectra of azide functionalized nanoparticles (NP-N_3), a-PEG, and PEG functionalized nanoparticles (NP-PEG)

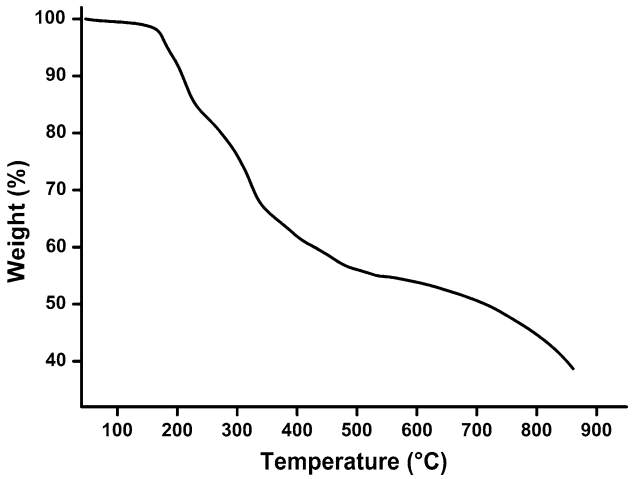

Fig. 8 Thermogravimetric analyses of PCL functionalized nanoparticles

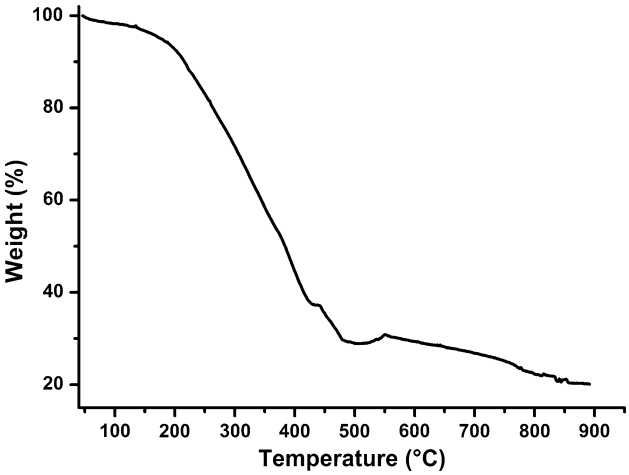

Fig. 10 Thermogravimetric analyses of PEG functionalized nanoparticles

through TGA analysis. The TGA curves for the PCL-coated Fe_3O_4 particles are reported in Fig. 8, depicting the variation of residual masses of the samples with temperature. The main weight loss stage occurred at around 200 °C can be attributed to the PCL decomposition. TGA analysis also indicated about 40% of the magnetite content.

Figure 9 depicted the ATR spectra of azide functional NPs (NP-N_3), a-PEG, and a-PEG functionalized NPs. The click reaction between the azide group and the alkyne group was confirmed by the disappearance of the alkyne peak around 2150 cm^{-1}. The functionalization is further confirmed by the presence of the typical peaks of PEG, such as C–O–C vibration around 1100 cm^{-1} and out-of-plane bending of the –CH of the chain at 960 cm^{-1}. The degree of functionalization of the magnetite particles was evaluated through TGA analysis. The TGA curves for the PEG-coated Fe_3O_4 particles is reported in Fig. 10, illustrating the variation of residual masses of the samples with temperature. The main weight loss stage occurred at around 225 °C and can be attributed to the PEG decomposition. This curve indicated that the magnetite content was about 20%, corresponding to an 80% PEG-shell content of the total weight. The higher shell content observed in the case of PEG may be due to the flexibility polyether chains which facilitate the click reaction more favorably.

Magnetization curves of PCL and PEG functionalized NPs are reported in Figs. 11 and 12, respectively. In both the cases, the hysteresis loop shows neither remanence nor coercivity, confirming that the polymer coated NPs have a superparamagnetic behavior suitable for biomedical applications.

The morphology of the coated NPs in aqueous solution has been investigated with TEM after transferring the aqueous solution to carbon coated copper grids. Figures 13

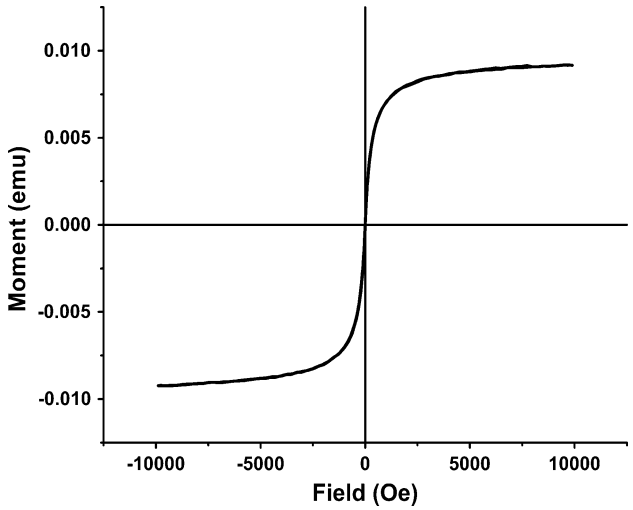

Fig. 11 Magnetization curve of PCL functionalized nanoparticles

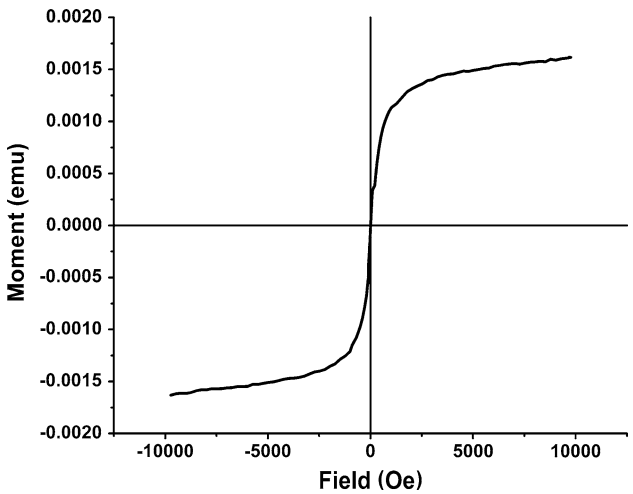

Fig. 12 Magnetization curve of PEG functionalized nanoparticles

and 14 show TEM micrographs of PCL coated NPs and PEG coated NPs, respectively. The presence of aggregates was probably due to the water droplet evaporation during TEM analysis. However, it should be noted that for both the samples the single particles are nanometric size range with an average size between 20 and 50 nm.

Conclusions

In this study, we described click chemistry methodology for the incorporation of biocompatible polymer chains to Magnetite nanoparticles (NPs). Thus, Magnetite nanoparticles were functionalized with bromine groups using (3-bromopropyl)trimethoxysilane, bromine groups were then substituted with azide groups using sodium azide.

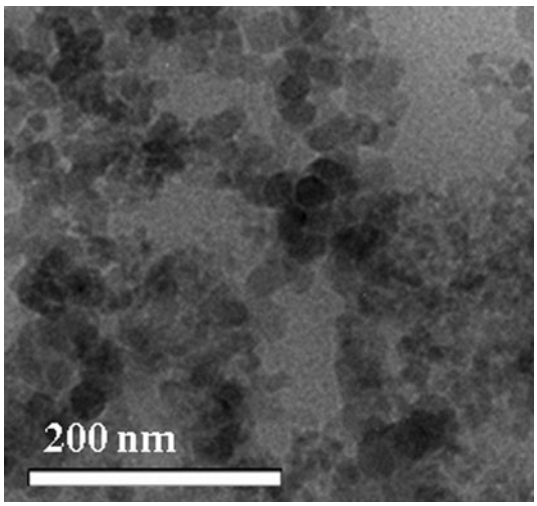

Fig. 13 TEM micrograph for aqueous dispersion of the PCL functionalized nanoparticles

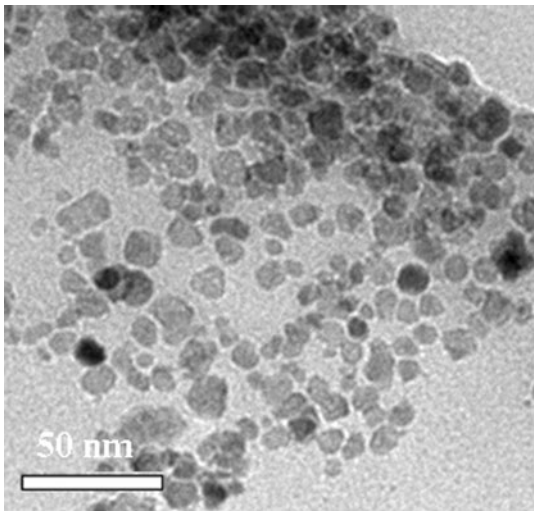

Fig. 14 TEM micrograph for aqueous dispersion of the PEG functionalized nanoparticles

The NPs were coated independently with PEG and PCL shell via click reaction by reacting alkyne groups of the polymers with azide groups available on the surface. ATR analysis confirmed the presence of a polymeric shell in both the cases. The shell content of the resulting composites was found to be 60 and 80% for PCL and PEG, respectively as determined by TGA analysis. The analysis of the magnetization curves show that the NPs have a superparamagnetic behavior which is crucial for endovenous administration in bio-medical application. TEM analysis confirmed the nanometric size with narrow size distribution of the coated NPs. Moreover, coating the Fe_3O_4 particles with PEG and PCL endowed the particles with excellent biocompatibility which is a mandatory request for medical

applications. Obviously, PEG chains impart additional hydrophilic character.

References

1. Purushotan S, Chang PEJ, Rumpel H, Kee IHC, Ng NTH, Chow PKH, Tan CK, Ramanujan RV (2009) Nanotechnology 20:305101
2. Gong P, Yu J, Sun H, Hong J, Zhao D, Xu D, Yao S (2006) J Apply Polym Sci 101:1283
3. Dilnawaz F, Singh A, Mohanty C, Sahoo SK (2010) Biomaterials 31:3694
4. Bicho A, Pec IN, Roque ACA, Cardoso MM (2010) Int J Pharm 399:80
5. Guanhua G, Rongrong S, Wenqing Q, Youguo S, Guofu X, Guanzhou Q, Xiaohe L (2010) J Mater Sci 45:3483. doi: 10.1007/s10853-010-4378-7
6. Zhang LY, Zhu XY, Sun HW, Chi GR, Xu JX, Sun YL (2010) Curr Apl Phys I 10:828
7. Bourlinos AB, Bakandritsos A, Georgakilas V, Tzitzios V, Petridis D (2006) J Mater Sci 41:5250. doi:10.1007/s10853-006-0041-8
8. Lee J, Lee Y, Youn LK, Na HB, Yu T, Kim H, Lee SM, Koo YM, Kwak JH, Park HG, Chang HN, Hwang M, Park JG, Kim J, Hyeon T (2998) Small 1:143
9. Arias JL, Reddy H, Couvreur P (2008) Langmuir 24:7512
10. Sonvico F, Dubernet C, Colombo P, Couvreur P (2005) Curr Pharm Des 11:2091
11. Alexiou C, Schmid RJ, Jurgons R, Kremer M, Wanner G, Bergemann C, Huenges E, Nawroth T, Arnold W, Parak FG (2006) Eur Biophys J 35:446
12. Arruebo M, Fernandez-Pacheco R, Ibarra MR, Santamaria J (2007) Nanotoday 2:22
13. Prijic S, Sersa G (2011) Radiol Oncol 45:1
14. Sun HW, Zhang LY, Zhu XJ, Kong CY, Zhang CL, Yao SD (2009) Sci China Ser B 52:69
15. Darwish MSA, Peuker U, Kunz U, Turek T (2011) J Mater Sci 46:2123. doi:10.1007/s10853-010-5048-5
16. Sun C, Lee JSH, Zhang M (2008) Adv Drug Delivery Rev 60:1252
17. Portet D, Denizot B, Rump E, Lejeune JJ, Jallet P (2001) J Colloid Interf Sci 238:37
18. Yang L, Peng XH, Wang YA, Wang X, Cao Z, Ni C, Karna P, Zhang X, Wood WC, Gao X, Nie S, Mao H (2009) Clin Cancer Res 15:4722
19. Neuberger T, Schopf B, Hofmann H, Hofmann M, von Rechenberg B (2005) J Magn Magn Mater 293:483
20. Kappiyoor R, Liangruksa M, Ganguly R, Puril IK (2010) J Appl Phys 108:4702
21. Frickel N, Messing R, Gelbrich T, Schmidt AM (2010) Langmuir 26:2839
22. Liu TY, Liu K, Liu DM, Chen SY, Chen IW (2009) Adv Funct Mater 19:616
23. Nan A, Turcu R, Craciunescu I, Pana O, Scharf H, Liebscher J (2009) J Polym Sci Part A 47:5397
24. Johnson JA, Finn MG, Koberstein JT, Turro NJ (2008) Macromol Rapid Commun 29:1052–1072
25. Durmaz YY, Sangermano M, Yagci Y (2010) J Polym Sci A 48:2862
26. Von Maltzahn G, Ren Y, Park JH, Min DH, Kotamraju VR, Jayakumar J, Fogal V, Sailor MJ, Erkki Ruoslahti SN (2008) Bioconjugate Chem 19:1570
27. Li LY, He WD, Li WT, Zhang KR, Pan TT, Ding ZL, Zhang BY (2010) J Polym Sci A 48:5018
28. Achatz DE, Heiligtag FJ, Li X, Link M, Wolfbeis OS (2010) Sens Actuators B 150:211
29. Amici J, Celasco E, Allia P, Tiberto P, Sangermano M (2011) Macromol Chem Phys 212:411
30. Zhiya M, Huizhou L (2007) Chin Partic 5:1
31. Stella B, Arpicco S, Peracchia MT, Desmaele D, Hoebeke J, Renoir M, D'Angelo J, Cattel L, Couvreur P (2000) J Pharm Sci 89:1452
32. Zablotskaya A, Segal I, Maiorov M, Zablotsky D, Mishnev A, Lukevics E, Shestakova I, Domracheva I (2007) J Magn Magn Mater 311:135
33. Mondini S, Cenedese S, Marinoni G, Molteni G, Santo N, Bianchi CL, Ponti A (2008) J Coll Interf Sci 322:173
34. Hyeon T (2003) Chem Commun 8:927
35. Lee Y, Lee J, Jin Bae C, Park J, Noh H, Park J, Hyeon T (2005) Adv Funct Mater 15:503